ELSEVIER

Physica C 295 (1998) 209–217

PHYSICA C

Lindemann criterion and vortex-matter phase transitions in high-temperature superconductors

V. Vinokur [a,*], B. Khaykovich [b], E. Zeldov [b], M. Konczykowski [c], R.A. Doyle [d], P.H. Kes [e]

[a] *Materials Science Division, Argonne National Laboratory, Argonne, IL 60439, USA*
[b] *Department of Condensed Matter Physics, The Weizmann Institute of Science 76100 Rehovot, Israel*
[c] *CNRS, URA 1380, Laboratoire des Solides Irradiés, École Polytechnique 91128 Palaiseau, France*
[d] *IRC in Superconductivity, University of Cambridge, Cambridge CB3 0HE, UK*
[e] *Kamerlingh Onnes Laboratorium, Rijksuniversiteit Leiden, P.O. Box 9506, 2300 RA Leiden, The Netherlands*

Received 30 September 1997; accepted 13 October 1997

Abstract

The vortex-matter in superconductors is generally believed to exist in two main phases, vortex-solid and vortex-liquid. Recent investigations of the phase diagram of anisotropic high-temperature superconductors indicate, however, the existence of at least three distinct phases: relatively ordered quasi-lattice, highly-disordered entangled vortex-solid, and a liquid phase. A theoretical analysis in terms of an extended Lindemann criterion provides a quantitative description of the resulting vortex-matter phase boundaries and the behavior of the transition lines with varying anisotropy and disorder. © 1998 Elsevier Science B.V.

1. Introduction

Vortex-matter in type-II superconductors provides a remarkable example of a condensed state with tunable parameters [1]. In contrast to conventional condensed matter systems, the density of constituent particles (magnetic flux-lines) and their interactions can be changed over several orders of magnitude in a controllable way, by simply varying the external magnetic field. In addition, experiments with high-temperature superconductors (HTSC) enable investigation of the important effects of thermal fluctuations. Vortex systems also offer a most convenient tool to investigate disordered media, another central issue in condensed matter physics. Recently developed experimental techniques allow for controlled introduction of both point and correlated defects in HTSC, providing a basis for systematic studies of the effects of disorder. Vortex matter is therefore a very rich field for both experimental and theoretical research.

The traditional view of a superconductor in the mixed state was that a homogeneous solid vortex lattice phase exists in a field interval between the lower critical field H_{c1}, where vortices start to penetrate into the superconductor, and the mean field upper critical field H_{c2}, above which superconductivity disappears. In the context of HTSC, however, the understanding of the enhanced role of thermal

* Corresponding author. Tel.: +1 630 252 3765; Fax: +1 630 252 7777.

PII S0921-4534(97)01795-4

fluctuations has lead to a prediction of vortex lattice melting and existence of two distinct vortex phases, vortex solid and vortex liquid [2]. However, the presence of quenched disorder and its interplay with thermal fluctuations appears to result in an even more complex mixed state phase diagram. In this paper we demonstrate that in the highly anisotropic HTSC in the presence of disorder there are at least three distinctly resolved phases of the vortex matter: a weakly disordered quasi-lattice, a highly disordered solid, and a liquid phase.

The structure of the vortex phases and the search for possible phase transitions in vortex matter have become one of the central issues in the study of the behavior of HTSC samples in a magnetic field. In general, structural defects and inhomogeneities in a material pin the vortex lines: vortices cannot move when the applied current is below a certain threshold called the critical current. In HTSC this pinning is usually weak due to the high operating temperatures, peculiar parameter values, and large anisotropy. This means that flux lines cannot be effectively pinned by one defect and an ensemble of defects is usually required to collectively pin the vortices [1]. It has therefore been suggested that the pinned lattice forms a glassy state which is characterized by divergent barriers for vortex motion. These barriers give rise to a strongly non-linear response to an infinitesimal driving force [1,3]. The common understanding before the advent of HTSC was that there is a unique disordered vortex-solid state, and that the main effect of varying the degree of material disorder would be a quantitative change in the size of the pinning correlation volume in which the ground state of the glassy phase is formed. Our understanding of the nature of the vortex solid phase has subsequently been extended by several recent experimental studies of HTSC, and in particular of the highly anisotropic $Bi_2Sr_2CaCu_2O_8$ (BSCCO) crystals. These results suggest the existence of at least two distinctly resolved solid phases of the vortex matter [4–9], and have stimulated several recent theoretical treatment [10–16] based on the generalization of the Lindemann criterion on the systems with disorder [17,18] and numerical simulations [19,20].

Fig. 1 shows a proposed phase diagram of a representative highly anisotropic HTSC (like BSCCO) in presence of weak point disorder. We

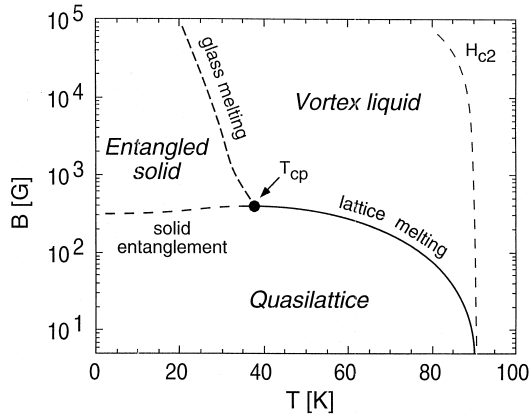

Fig. 1. Schematic phase diagram (on a logarithmic scale) of highly anisotropic HTSC in the mixed state based on experimental results in BSCCO. The vortex-liquid state can be either liquid of vortex lines or a gas of vortex pancakes. The liquid phase is determined by $T > \mathscr{E}_{pin}, \mathscr{E}_{el}$. The quasi-lattice phase is a rather ordered solid state characterized by $\mathscr{E}_{el} > T, \mathscr{E}_{pin}$. The entangled solid is a highly disordered vortex-solid phase with $\mathscr{E}_{pin} > T, \mathscr{E}_{el}$. The quasi-lattice melts (or sublimates) through a first-order lattice-melting transition described by $\mathscr{E}_{el} = T$. The disorder-driven solid-entanglement transition occurs at lower temperatures at fields characterized by $\mathscr{E}_{el} = \mathscr{E}_{pin}$. Melting of the entangled solid occurs at the glass melting transition where $\mathscr{E}_{pin} = T$. The three transition lines merge at the critical point T_{cp}, where the elastic, pinning, and thermal energies are comparable.

distinguish three main vortex phases: the high-temperature high-field vortex-liquid and two vortex-solid phases which are hereafter referred to as the low-field quasi-lattice and the high-field entangled-solid. As we show below, the existence of two distinct solid phases is the result of point disorder. Elastic interactions govern the structure of the vortex-solid at low fields, forming a quasi-lattice in which a well-defined lattice structure is preserved and long range order is only weakly destroyed. At higher fields disorder dominates and vortex–pin interactions result in an entangled solid where elementary cells of vortex lattice are twisted and dislocations proliferate [10,12,13,19,20]. An important question is the order of the thermodynamic transitions between the various phases. Due to its long range order, the quasi-lattice is expected to melt through a first-order lattice-melting transition at high temperatures (Fig. 1). Extensive experimental studies including transport [21–27], magnetization [28–31], AC susceptibility [32,33], and calorimetric [34] methods, have estab-

lished the existence of such a first-order transition in clean YBCO and BSCCO crystals. The entangled solid, on the other hand, should melt through a continuous glass-melting transition [1,3,35,36]. The solid entanglement transition was recently shown to be very sharp [8] and is possibly a second-order solid–solid transition.

In this paper we describe a phenomenological model which enables us to derive the three transition lines using a unified simple approach developing and extending the approach of [10–16]. We pay a special attention to application of the model to layered superconductors, which was missing in the above studies, and compare the results with the experimental data on BSCCO single crystal. The model is based on the Lindemann criterion which is generalized [17,18] to apply to a system containing disorder. The vortex–vortex interactions are accounted for by a mean-field-like 'cage model' description [17]. Our analysis is able to describe both the experimentally derived phase diagram and the recently observed shifts of the transition lines with anisotropy [8,37] and disorder [9] rather well.

2. Theoretical approach

The classical Lindemann criterion describes the melting transition in terms of a mean square thermal displacement of the constituent particles. In the context of a vortex-lattice, melting occurs when the mean thermal displacements of vortex-lines from their equilibrium positions become a certain fraction of the vortex-lattice spacing a_0, $\langle u^2 \rangle = c_L^2 a_0^2$, where c_L is the Lindemann number which for the vortex-lattice is between 0.1–0.2 [1]. This Lindemann criterion can be described in terms of characteristic energies: the vortex lattice melts when the energy of thermal fluctuations becomes equal to the elastic energy barriers keeping vortices near their equilibrium positions in the lattice:

$$T = \mathscr{E}_{el}. \tag{1}$$

In the presence of point disorder, competition between the elastic tension of the vortex and the random field induced by defects gives rise to a rugged energy landscape and rough vortex paths. These disordered configurations contribute to the entropic part of the vortex free energy [18]. The characteristic energy, $\mathscr{E}_{pin}$, which describes the depth of the disorder-induced potential wells for vortex lines, is called the pinning energy. With this additional energy coming into play one can generalize the Lindemann criterion for a disordered system by including $\mathscr{E}_{pin}$ into the energy balance [17,18]. As a result, all three lines on the phase diagram of Fig. 1 can be obtained by balancing the appropriate characteristic energies. The first-order melting transition of the quasi-lattice occurs when the temperature matches the elastic barriers as given by Eq. (1). At low temperatures the influence of quenched disorder effectively increases with increasing magnetic field as described below, and at some characteristic field the disorder-induced positional entropy dominates the elastic barriers. This causes the transition from the quasi-lattice to the highly-disordered entangled vortex-solid. The solid-entanglement transition field B_E is thus determined by

$$\mathscr{E}_{pin} = \mathscr{E}_{el}. \tag{2}$$

Finally, melting of the entangled solid occurs at temperatures where the pinning energy matches the energy of thermal fluctuations [18]:

$$T = \mathscr{E}_{pin}. \tag{3}$$

In the vicinity of the critical point, T_{cp}, where the three lines merge, all three energy scales have to be taken into account.

3. The solid-entanglement transition

The essential aspects of single vortex pinning by weak disorder can be summarized as follows [1]. Being an elastic object, the vortex line accommodates itself to the random landscape and follows a rough optimal path determined by the balance between the elastic and pinning energies. The geometry of these optimal paths is characterized by their *roughness*, $u(L) = \langle [\boldsymbol{u}(L) - \boldsymbol{u}(0)]^2 \rangle^{1/2}$, where $\langle \dots \rangle$ indicates averaging over both thermal and quenched disorder, $\boldsymbol{u}$ is the transverse displacement of the vortex line, and L is the distance along the line. At large distances $u(L) \approx \xi (L/L_c)^{\zeta}$, where $\zeta \simeq 3/5$ is the roughness exponent, $L_c = (\epsilon_1^2 \xi^4 / \gamma)^{1/3}$ is the

Larkin pinning length, and $\epsilon_1 = \epsilon^2\epsilon_0$ is the vortex line tension. Here ϵ is the anisotropy parameter, $\epsilon_0 = \Phi_0^2/(4\pi\lambda)^2$, Φ_0 is the flux quantum, λ is the London penetration depth, ξ is the coherence length, and γ is the variance of the strength of point disorder. The pinning length L_c is the size of a coherently pinned vortex segment and defines a length over which low-lying metastable vortex states are formed. The characteristic pinning energy of a vortex segment of length $L > L_c$ is $\mathscr{E}_{pin}(L) \simeq T_{dp}(L/L_c)^{2\zeta-1}$, where T_{dp} is the pinning energy of the coherently pinned segment, while the characteristic energy for $L < L_c$ is $\mathscr{E}_{pin}(L) \simeq \sqrt{\gamma L}$.

From the point of view of vortex lattice stability the effect of point defects is two-fold. On the one hand, defects localize the vortex line within low lying metastable states which are separated from neighboring metastable states by barriers of order $\mathscr{E}_{pin}$, and thus harden the vortex solid. On the other hand, pinning stimulates transverse wandering of vortex lines. These frozen-in wanderings can destroy long-range order of the vortex lattice in a manner analogous to the action of the thermal noise and may generate topological defects in the lattice.

The structure of the vortex solid is determined by a competition between the pinning and elastic energies. We consider a representative vortex as being confined in the cage of transverse size a_0 due to the rest of the lattice. The total elastic energy of the vortex is a sum of the confining harmonic potential of the cage and the tilting energy of the vortex line, $\mathscr{E}_{el} = c_{66}u^2L + \epsilon_1(u^2/L)$, where u and L are the transverse and longitudinal sizes of vortex distortion respectively, and $c_{66} \simeq \epsilon_0/4a_0^2$ is the vortex-lattice shear modulus. Minimization of the elastic energy with respect to L gives the characteristic size of the longitudinal fluctuation L_0 as

$$L_0 = \sqrt{\epsilon_1/c_{66}} \simeq 2\varepsilon a_0. \tag{4}$$

The characteristic longitudinal length L_0 defines the size of elastic screening of local distortions of the vortex line in the cage. In other words, local elastic fluctuations of the caged vortex separated by distances $L \gg L_0$ become independent. L_0 can therefore be viewed as the longitudinal size of the elastic cage. The characteristic elastic energy of the vortex in the cage thus becomes $\mathscr{E}_{el} = \varepsilon\epsilon_0 u^2/a_0$. Near the solid-entanglement transition we expect $u^2 = c_L^2 a_0^2$, and therefore

$$\mathscr{E}_{el} = \varepsilon\epsilon_0 c_L^2 a_0. \tag{5}$$

The characteristic pinning energy of the representative vortex line in the cage depends on the relation between L_0 and the pinning length L_c. If $L_c > L_0$, the pinning energy in the cage is $\mathscr{E}_{pin} \simeq \sqrt{\gamma L_0} \simeq (2\gamma\varepsilon a_0)^{1/2}$. In the opposite limit, a vortex line has enough room to follow the optimal path consisting of many segments of the length L_c, and a rough vortex configuration with the mean lateral displacement $u \propto (L_0/L_c)^{\zeta}$ forms within the cage. In what follows we restrict ourselves to this more practical limit [10]. If $s < L_c < L_0$, where s is the interlayer spacing the pinning energy becomes

$$\mathscr{E}_{pin} = T_{dp}(L_0/L_c)^{2\zeta-1}, \tag{6}$$

where $T_{dp} = (\gamma\epsilon_1\xi^2)^{1/3}$ is the depinning temperature of a single vortex line [1]. In highly anisotropic superconductors like BSCCO ($\varepsilon \approx 1/100$) L_c becomes much smaller not only than the cage longitudinal size L_0, but also than the interlayer spacing s. In this case the pancake vortices are pinned individually and the pinning energy per cage assumes the form:

$$\mathscr{E}_{pin} = U_p(L_0/s)^{2\zeta-1}, \tag{7}$$

where $U_p = \pi\sqrt{\gamma s}$ is one pancake pinning energy.

The important observation here is that while the elastic energy per cage decreases with field as $\mathscr{E}_{el} \propto B^{-1/2}$, the pinning energy decays only as $\mathscr{E}_{pin} \propto B^{-1/10}$. Therefore elastic forces dominate at low fields, and as a result a rather ordered quasi-lattice is formed. At elevated fields, however, the disorder induced lateral displacements distort the cages and break up the quasi-lattice configuration. The transition from almost regular to strongly distorted vortex configuration can be visualized as follows.

In the quasi-lattice phase the most preferable vortex trajectories are those that slightly wiggle about the equilibrium positions in a perfect lattice as represented at Fig. 2a. At low field, the random disorder weakly perturbs the parabolic potential of the cage, as shown schematically in Fig. 2b. Then the local minima corresponding to the metastable states lo-

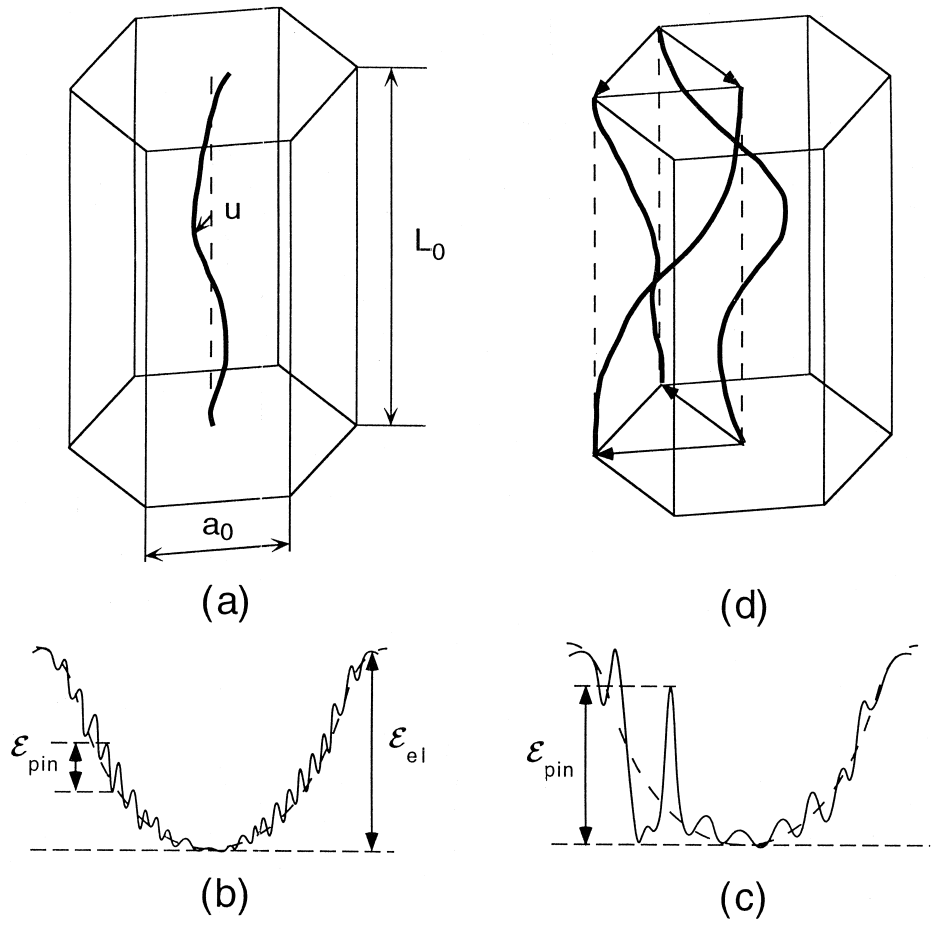

Fig. 2. Schematic behavior of a vortex-line in the cage potential due to neighboring vortices perturbed by point disorder. (a) Representative vortex line wondering within the cage due to action of point defects. (b) At low fields below the entanglement transition ($B < B_E$) the pinning energy $\mathscr{E}_{pin}$ due to disorder is much smaller than the elastic energy $\mathscr{E}_{el}$. (c) With increasing field the pinning energy becomes relatively more important resulting in rougher potential landscape. At the entanglement transition field $B = B_E$ the potential displays two competing minima of the same depth due to the competition of cage and pinning energy, as follows from Eq. (2). (d) At fields $B > B_E$ the enhanced relative wandering of the vortices due to point disorder results in quenched entanglement and permutations of neighboring vortices. Local twisting of the cage gives rise to the formation of dislocations.

cated far from the center of the cage are not occupied. As field is increased the potential landscape becomes more rough. The meaning of Eq. (2) is that at the solid-entanglement transition the depth of the potential minima due to disorder becomes comparable to the depth of the main valley as represented in Fig. 2c. These minima are located at distances of the order of a_0 from the center, and become more favorable with increasing field. As a result, at $B = B_E$, the vortex line can switch its position abruptly to a trajectory which is considerably displaced from its original position near the perfect lattice site. Another way to think about the transition is to noting that the mean lateral deviations of the best trajectories accumulated over a distance equal to L_0 become of the order of the lattice constant a_0 at $B = B_E$. This gives rise to twist deformations in the vortex lattice. Consequently, permutations of neighboring vortices occur and an entangled vortex configuration is formed as shown schematically in Fig. 2d. Note that the

region where two neighboring vortices switch their positions is essentially an element of a dislocation lying in the *ab*-plane. One can therefore expect that at this solid-entanglement transition closed loops of vortex transmutations will appear, i.e. dislocation loops will proliferate. A similar description has recently been suggested in Refs. [10,12,13,19,20]. We emphasize, however, that there is currently no detailed theory for the entangled solid phase. In particular, the origin of the enhanced pinning which is observed in this phase and which gives rise to the second magnetization peak [6–9] requires further study.

By comparing the pinning and elastic energies (Eqs. (5)–(7)) we now derive the solid entanglement transition field

$$B_E = \begin{cases} B_0 \left(\dfrac{T_0}{T_{dp}} \right)^{\frac{2\zeta}{1-\zeta}}, & s < L_c < L_0 \\ B_{2D} \left(\dfrac{U_{pc}}{U_p} \right)^{1/(1-\zeta)}, & L_c < s < L_0 \end{cases} \tag{8}$$

where $B_0 = c_L^2 \Phi_0 / \xi^2$, $T_0 = c_L \varepsilon \epsilon_0 \xi / 2$, and $U_{pc} = c_L^2 s \epsilon_0 / \pi$. $B_{2D} = \Phi_0 \varepsilon^2 / s^2$ is the 3D–2D crossover field. Taking the typical parameters for YBCO ($\lambda =$ 2000 Å, $\xi = 20$ Å, $\varepsilon = 1/7$, $s < L_c < L_0$) one finds $T_0 \approx 20$ K. The exact value of the depinning temperature is not known at present, but the expected T_{dp} lies in the interval 20–60 K. As a result the solid entanglement transition in YBCO is expected to occur at very high fields, $B_E \simeq B_0 \approx 20$ T. In BSCCO $L_c < s$ and the value of B_E is very sensitive to anisotropy and to the magnitude of the Lindemann number c_L which is not necessarily equal to its value for the lattice melting transition. Assuming the usual value $c_L \approx 0.16$ and taking $\varepsilon = 1/100$ we obtain $U_{pc} \approx 7$ K, $B_{2D} = 900$ G, and estimating the pancake pinning energy in BSCCO as $U_p \approx T_{dp} \approx 10$ K we arrive at $B_E \approx 370$ G in a very good agreement with the experimentally observed values [4–9,37]. B_E is predicted to decrease with crystal anisotropy, $B_E \propto \varepsilon^2$, in agreement with the experiments [8,37]. The important result here is, however, that B_E decreases with increasing disorder [6,7,9], due to an increase of U_p, as demonstrated in Fig. 3 for an electron irradiated BSCCO crystal.

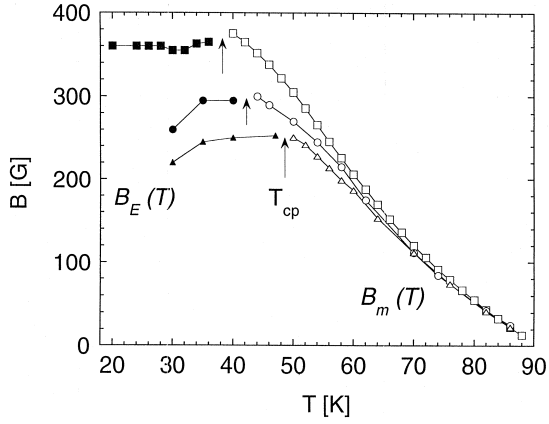

Fig. 3. Experimental phase diagram of BSCCO in presence of weak point disorder as inferred from local magnetization measurements [9]. Open symbols indicate the location of the first-order transition, $B_m(T)$, and the filled symbols show the position of the solid entanglement transition $B_E(T)$, square – as-grown crystal, circle – after 2.5 MeV electron irradiation to a dose of 3×10^{18} cm^{-2}, triangle – after 6×10^{18} cm^{-2} electron irradiation. The enhanced point disorder induced by electron irradiation results in a shift of the solid entanglement transition $B_E(T)$ to lower fields accompanied by a downward bending of the melting line $B_m(T)$. The critical point T_{cp} is shifted to higher temperatures with increased disorder.

When deriving the transition field of Eq. (8) we neglected the electromagnetic interactions between pancakes and for simplicity accounted for their Josephson coupling only. Another important note is that weak disorder, such that $U_p < U_{pc}$, cannot cause solid entanglement. Indeed, according to Eq. (8) $U_p < U_{pc}$ implies $B_E > B_{2D}$, and the transition should fall into the 2D domain. Bearing in mind that the condition $B > B_{2D}$ is equivalent to $L_0 < s$, one notes that the cage is now confined to a single layer and, accordingly, holds only one pancake. Then the elastic energy stored in the cage near the supposed transition is merely U_{pc} and the corresponding pinning energy in the cage (i.e. per pancake) is U_p. For the entanglement to occur these two energies have to match, in conflict with the assumed condition $U_p < U_{pc}$. We therefore conclude that solid entanglement may occur only if disorder is sufficiently strong, $U_p > U_{pc}$ and that the transition itself falls in this case into the 3D domain, $B_E < B_{2D}$. A further obser-

vation is that at low temperatures $\mathscr{E}_{pin}(T)$ is constant which results in a flat $B_E(T)$ as given by Eq. (8). However, with increasing temperature, $\mathscr{E}_{pin}(T)$, decreases due to thermal smearing of the pinning potential. As a result, following Eq. (2), $B_E(T)$ is expected to show an upturn at intermediate temperatures, as is indeed observed in BSCCO crystals with various anisotropies [8,37] and also indicated in Fig. 3.

4. Glass and lattice melting

To complete the description of the proposed phase diagram in Fig. 1 we now turn to the melting transitions. In the quasi-lattice phase the effective pinning at high temperatures is very weak. Weak disorder distorts the lattice only on length scales much larger than the inter-vortex spacing [1]. Melting, on the other hand, is governed by the vortex fluctuations on short scales of the order of a_0. As a result the first-order melting line is determined by the conventional Lindemann relation as in Eq. (1):

$$B_m(T) \simeq \frac{\Phi_0 \varepsilon^2 \epsilon_0^2 c_L^4}{T^2}. \quad (9)$$

As one moves along the lattice melting line to lower temperatures and higher fields the role of disorder increases. This results in the termination of the first-order transition at the critical point T_{cp}. At T_{cp} the lattice melting line splits into the solid entanglement (Eqs. (2) and (8)) and the glass melting (Eq. (3)) transitions as shown in Fig. 1. Evidence which may be consistent with a continuous glass melting transition has been observed both in YBCO and BSCCO samples [35,36]. Further, suppression of the first-order melting was demonstrated by introduction of point defects into an untwinned YBCO crystal via electron irradiation [38]. However, the detailed mechanism of freezing of the vortex liquid into the entangled solid remains controversial and appeals for further experimental and theoretical study.

Although a rigorous description of the transition lines in the vicinity of the critical point T_{cp} is not available at present, a rough estimate of the position of the critical point can be obtained by extrapolating the three transition lines to the point where all three characteristic energies are equal:

$$T_{cp} = \mathscr{E}_{el}(B_E) = \mathscr{E}_{pin}(B_E) \simeq \pi U_{pc} \left(\frac{U_p}{U_{pc}} \right)^{5/4}, \quad (10)$$

which with the chosen values of parameters gives $T_{cp} \approx 35$ K for BSCCO in a good agreement with experiment [8,9,28,37]. Upon increasing disorder the critical point is expected to shift towards higher temperatures, as indeed observed in Fig. 3.

Qualitatively we speculate that the effects of disorder-induced fluctuations and thermal fluctuations sum so that for any given field the melting occurs at a lower temperature relative to the clean limit with no $\mathscr{E}_{pin}$. Thus weak point disorder should result in a downward shift and in flattening of the lattice melting as T_{cp} is approached from above. Fig. 3 clearly shows this behavior in BSCCO crystals [8,9,28,37]. The flattening of the first-order transition line $B_m(T)$ near T_{cp} is observed in as-grown crystals due to intrinsic disorder. Incremental increase of point disorder through electron irradiation results in a downward shift of $B_m(T)$ in the vicinity of T_{cp}, and flattening towards the solid-entanglement transition sets in at progressively higher temperatures.

It should be emphasized that the description of the different vortex phases above and as shown in Fig. 1 is not unique. If the role of pinning is substantially enhanced with respect to thermal fluctuations, the critical point T_{cp} can be shifted all the way up to the critical temperature, and the first-order melting of the quasi-lattice disappears. In this case the quasi-lattice transforms with increasing field into the entangled solid phase at all temperatures, as reported recently for $Nd_{1.85}Ce_{0.15}CuO_{4-\delta}$ crystals [39].

Finally, an interesting test of the solid entanglement transition is incorporation of a low dose of columnar defects by heavy ion irradiation. This is expected to confine transverse vortex fluctuations [17], thus preventing vortex entanglement. We can estimate the minimum density of columnar defects, n, necessary to suppress the entanglement by requiring $\mathscr{E}^c_{pin} \geq \mathscr{E}^p_{pin}$. Here the upper index p stands for point disorder and c for correlated disorder due to columnar defects. The pinning energy of a pancake stack of length εa_0 centered around a given columnar defect can be estimated as $\varepsilon a_0 \epsilon_0$. Taking into

account that only a fraction of vortices is trapped near columnar defects we arrive at $\mathscr{E}_{\rm pin}^{\rm c} \simeq \varepsilon n a_0^3 \epsilon_0$. Since at the entanglement transition $\mathscr{E}_{\rm pin}^{\rm p} \simeq \varepsilon \epsilon_0 c_{\rm L}^2 a_0$, one arrives at the condition for the columnar defects to suppress the quenched entanglement as

$$B_\Phi > c_{\rm L}^2 B_{\rm E}, \tag{11}$$

where $B_\Phi = n\Phi_0$ is the so called matching field. For $c_{\rm L} \approx 0.16$ and $B_{\rm E} \approx 400$ G we find that B_Φ should exceed 12 G in order to suppress the quenched entanglement transition. Such a suppression of the entanglement transition at very low doses of columnar defects was recently observed in BSCCO crystals [9].

5. Conclusion

We have presented a qualitative description of the phase diagram of anisotropic superconductors with transition lines derived from the Lindemann criterion generalized on the systems with disorder. Several notes are in order. First of all one has to bear in mind that Lindemann criterion, being a powerful phenomenological tool for evaluation of the position of the supposed transitions, tells us nothing about the nature of the resulting phases nor can it even guarantee the existence of the transition at all. In this respect the creation of the rigorous theory of the solid entanglement transition discussed above remains an appealing task for future research. To be fair, one should note at this point that to the best of our knowledge no theory exists for the phase transition in a real 3D system. One of the most long-standing problems in the field of statistical mechanics and physics of phase transition is the problem of the conventional melting. The use of the Lindemann criterion in this case is based rather on our deep belief that melting does exist than on any rigorous theory. One can consider thus a study of the solid entanglement as a part of massive efforts towards the general theory of phase transformations. A less philosophical and more technical point is that for the more accurate description of the transition line magnetic interactions between pancakes should be taken into account. The detailed calculations are somewhat technical and go beyond the scope of this paper, so we will present them in the forthcoming publication [40]. And the last but not least important note is that the quantitative theory of the entangled solid itself remain an uncompleted task. In particular, the basic observation, the abrupt increase of the apparent critical current (or persistent current) did not receive a quantitative explanation. On the qualitative level one can understand this phenomenon as a result of the combined action of two effects: (i) increase of the true critical current due to availability of more deep pinning potential wells for each pancake and (ii) the suppression of pancake creep due to trapping by these low-lying pinning states. The former effect gives rise to an increase in the critical current approximately by a factor of $\sqrt{\ln(a/\xi)/\ln(c_{\rm L} a/\xi)}$ (see [40] for more detail), providing thus a jump in $J_{\rm c}$ by a factor of ≈ 1.5 for BSCCO parameters. The creep suppression can lead to a further increase of the jump in the persistent current, but the quantitative theory of this effect remains the task for future research.

Acknowledgements

Helpful discussions with D.R. Nelson, A. Koshelev, G. Blatter, V.B. Geshkenbein and M.W. McElfresh are gratefully acknowledged. This work was supported by the US Department of Energy, BES-Material Sciences, under Contract No. W-31-109-ENG-38, by the Israel Science Foundation, by the US-Israel Binational Science Foundation, and by the Albert Einstein Minerva Center for Theoretical Physics.

References

[1] G. Blatter et al., Rev. Mod. Phys. 66 (1994) 1125.
[2] D.R. Nelson, Phys. Rev. Lett. 60 (1988) 1975.
[3] M.P.A. Fisher, Phys. Rev. Lett. 62 (1989) 1415.
[4] R. Cubitt et al., Nature 365 (1993) 407.
[5] S.L. Lee, P. Zimmermann, H. Keller, M. Warden, I.M. Savić, R. Schauwecker, D. Zech, R. Cubitt, E.M. Forgan, P.H. Kes, T.W. Li, A.A. Menovsky, Z. Tarnawski, Phys. Rev. Lett. 71 (1993) 3862.
[6] N. Chikumoto, M. Konczykowski, N. Motohira, A.P. Malozemoff, Phys. Rev. Lett. 69 (1992) 1260.
[7] N. Chikumoto, M. Konczykowski, N. Motohira, K. Kishio, K. Kitazawa, Physica C 185–189 (1991) 2201.

[8] B. Khaykovich, E. Zeldov, D. Majer, T.W. Li, P.H. Kes, M. Konczykowski, Phys. Rev. Lett. 76 (1996) 2555.
[9] B. Khaykovich, M. Konczykowski, E. Zeldov, R.A. Doyle, D. Majer, P.H. Kes, and T.W. Li, Phys. Rev. B 56 (1997) R517; Czech J. Phys. 46, Suppl. S6 (1996) 3218.
[10] D. Ertas, D.R. Nelson, Physica C 272 (1996) 79.
[11] V. Vinokur, B. Khaykovich, E. Zeldov, unpublished.
[12] J. Kierfeld, preprint cond-mat/9609045, submitted to Physica C.
[13] T. Giamarchi, P. Le Doussal, Phys. Rev. B 55 (1997) 6577.
[14] Y.Y. Goldshmidt, Phys. Rev. B 56 (1997) 2800.
[15] R. Ikeda, J. Phys. Soc. Jpn. 65 (1996) 3998.
[16] D.S. Fisher, Phys. Rev. Lett. 78 (1997) 1964.
[17] D.R. Nelson, V. Vinokur, Phys. Rev. B 48 (1993) 13060.
[18] A.I. Larkin, V.M. Vinokur, Phys. Rev. Lett. 75 (1995) 4666.
[19] M.J.P. Gingras, D.A. Huse, Phys. Rev. B 53 (1996) 15193.
[20] S. Ryu, A. Kapitulnik, S. Doniach, Phys. Rev. Lett. 77 (1996) 2300.
[21] H. Safar, P.L. Gammel, D.A. Huse, D.J. Bishop, J.P. Rice, Phys. Rev. Lett. 69 (1992) 824.
[22] H. Safar, P.L. Gammel, D.A. Huse, D.J. Bishop, W.C. Lee, J. Giapintzakis, D.M. Ginsberg, Phys. Rev. Lett. 70 (1993) 3800.
[23] W.K. Kwok, S. Fleshler, U. Welp, V.M. Vinokur, J. Downey, G.W. Crabtree, M.M. Miller, Phys. Rev. Lett. 69 (1992) 3370.
[24] W.K. Kwok, J. Fendrich, S. Fleshler, U. Welp, J. Downey, G.W. Crabtree, Phys. Rev. Lett. 72 (1994) 1092.
[25] D.T. Fuchs, E. Zeldov, D. Majer, R.A. Doyle, T. Tamegai, S. Ooi, M. Konczykowski, Phys. Rev. B 54 (1996) R796.
[26] D.T. Fuchs, R.A. Doyle, E. Zeldov, D. Majer, W.S. Seow, R.J. Drost, T. Tamegai, S. Ooi, M. Konczykowski, P.H. Kes, Phys. Rev. B 55 (1997) R6156.
[27] S. Watauchi, H. Ikuta, J. Shimoyama, K. Kishio, Physica C 259 (1996) 373.
[28] E. Zeldov, D. Majer, M. Konczykowski, V.B. Geshkenbein, V.M. Vinokur, H. Shtrikman, Nature 375 (1995) 373.
[29] H. Pastoriza, M.F. Goffmann, A. Arribére, F. de la Cruz, Phys. Rev. Lett. 72 (1994) 2951.
[30] R. Liang, D.A. Bonn, W.A. Hardy, Phys. Rev. Lett. 76 (1996) 835.
[31] U. Welp, J.A. Fendrich, W.K. Kwok, G.W. Crabtree, B.W. Veal, Phys. Rev. Lett. 76 (1996) 4809.
[32] R.A. Doyle, D. Liney, W.S. Seow, A.M. Campbell, Phys. Rev. Lett. 75 (1995) 4520.
[33] N. Morozov, E. Zeldov, D. Majer, M. Konczykowski, Phys. Rev. B 54 (1996) R3784.
[34] A. Schilling, R.A. Fisher, N.E. Phillips, U. Welp, D. Dasgupta, W.K. Kwok, G.W. Crabtree, Nature 382 (1996) 791.
[35] R.H. Koch, V. Foglietti, W.J. Gallagher, G. Koren, A. Gupta, M.P.A. Fisher, Phys. Rev. Lett. 63 (1989) 511.
[36] H. Safar, P.L. Gammel, D.J. Bishop, D.B. Mitzi, A. Kapitulnik, Phys. Rev. Lett. 68 (1992) 2672.
[37] T. Hanaguri, T. Tsuboi, A. Maeda, T. Nishizaki, N. Kobayashi, Y. Kotaka, J. Shinoyama, K. Kishio, Physica C 256 (1995) 111.
[38] J.A. Fendrich, W.K. Kwok, J. Giapintzakis, C.J. Van der Beek, V.M. Vinokur, S. Fleshler, U. Welp, H.K. Vishwanathan, G.W. Crabtree, Phys. Rev. Lett. 74 (1995) 1210.
[39] D. Giller, A. Shaulov, R. Prozorov, Y. Abulafia, Y. Wolfus, L. Burlachkov, Y. Yeshurun, preprint.
[40] A.E. Koshelev, V.M. Vinokur, to be published.